

A stabilised mixed method applied to compressible fluid flow: The stationary case

Dedicated to Prof. R. Rodríguez, on the occasion of his 65 birthday

TOMÁS P. BARRIOS ^{*}, EDWIN M. BEHRENS [†] and ROMMEL BUSTINZA [‡]

Abstract

This article is concerned with a compressible fluid flow with non-homogeneous Dirichlet boundary condition. First, we reformulate the problem in its dual mixed form, and then we study its corresponding well posedness. Next, in order to circumvent the well known Babuška-Brezzi condition, we analyse a stabilised formulation of the resulting approach. Additionally, we endow the scheme with an a posteriori error estimator that is reliable and efficient. Finally, we provide numerical experiments that illustrate the performance of the corresponding adaptive algorithm and support its use in practice.

Mathematics Subject Classifications (1991): 65N15, 65N30, 65N50

Key words: A posteriori error estimates, augmented mixed formulation, Ritz projection of the error.

1 Introduction

In [15] a dual mixed finite element method for the incompressible fluid flow was introduced and analysed. The approach there follows the ideas developed in [14], i.e., the incompressible fluid flow is reformulated using the new variable so-called pseudostress, which is in relation with the pressure and gradient of the velocity. The main advantage of this new variable is the accurate approximation to physical quantities such as the stress and vorticity, allowing to use the pair of conforming Raviart-Thomas with discontinuous polynomial as the finite element space. Furthermore, in order to obtain more flexibility in the finite element spaces, the stabilisation of this approach has been studied in [19], and additionally its corresponding extension to quasi Newtonian flows and Brinkman model were developed in [20] and [4], respectively.

^{*}Departamento de Matemática y Física Aplicadas, Universidad Católica de la Santísima Concepción, Casilla 297, Concepción (Chile). E-mail: tomas@ucsc.cl

[†]Departamento de Ingeniería Civil, Universidad Católica de la Santísima Concepción, Casilla 297, Concepción (Chile). E-mail: ebehrens@ucsc.cl

[‡]Centro de Investigación en Ingeniería Matemática (CI²MA) & Departamento de Ingeniería Matemática, Universidad de Concepción, Casilla 160-C, Concepción (Chile). E-mail: rbustinz@ing-mat.udec.cl.

On the other hand, studying linear elasticity problem, in [3] we present an alternative a posteriori error estimator to the previous one developed in [12]. This approach is based on the Ritz projection of the error (see [11]). As result, in the case of homogeneous Dirichlet boundary condition, we obtain a reliable and local efficient a posteriori error estimator, that only requires the computation of four residuals per element, which is a low computational cost comparing with the eleven terms included in the estimator developed in [12] for the same case. This kind of a posteriori error estimator, at least, have been developed satisfactorily in different directions, for example, the Poisson problem is studied in [11], Darcy flow in [8] and [9], the Brinkman model in [5], linear elasticity in [3] and recently the Oseen equations in [10].

Then, our interest in this article is to study a compressible fluid flow using a stabilised mixed approach. In order to describe as clear as possible the stabilisation procedure, we begin by applying a dual mixed approach, where the well posedness is consequence of the standard Babuška-Brezzi theory. After that, we include the analysis of a stabilised formulation, which allows us to expand the choice of stable pairs that could be used to approximate the solution. In addition, and strongly motivated by the reduction of computational cost obtained with the a posteriori error estimator based on Ritz projection of the error, we endowed the new approach with an estimator of this type, which have only five terms, thus it has a low computational cost.

In what follows, in order to describe the model of interest, we let Ω be a bounded and simply connected domain in \mathbb{R}^2 with polygonal boundary Γ . Then, given the source terms $\tilde{f} \in L_0^2(\Omega)$, $\mathbf{f} \in [L^2(\Omega)]^2$ and $\mathbf{g} \in [H^{1/2}(\Gamma)]^2$, we look for the velocity (vector field) \mathbf{u} and the pressure (scalar field) p such that

$$-\nu\Delta\mathbf{u} + \nabla p = \mathbf{f} \quad \text{in } \Omega, \quad \text{div}(\mathbf{u}) = \tilde{f} \quad \text{in } \Omega, \quad \text{and } \mathbf{u} = \mathbf{g} \quad \text{on } \Gamma, \quad (1)$$

where $\nu > 0$ is the fluid viscosity of the flow and the datum \mathbf{g} satisfies the compatibility condition $\int_{\Gamma} \mathbf{g} \cdot \mathbf{n} = 0$, with \mathbf{n} being the unit outward normal at Γ . In addition, for uniqueness purposes, we seek $p \in L_0^2(\Omega) := \{q \in L^2(\Omega) : \int_{\Omega} q = 0\}$.

The rest of the paper is organised as follows. In Section 2, we analysed the dual mixed variational formulation for the compressible fluid flow in the plane, the corresponding Galerkin scheme and the simplest finite element subspaces that can be used. Section 3 is concerned with a stabilisation of the dual mixed approach, whereas in Section 4, we develop an a posteriori error analysis and deduce a new a posteriori error estimate. Finally, in Section 5 we provide several numerical experiments that support the use of our a posteriori error estimates in practice.

We end this section with some notations to be used throughout the paper. Given a Hilbert space H , we denote by H^2 (resp., $H^{2 \times 2}$) the space of vectors (resp., square tensors) of order 2 with entries in H . Given $\boldsymbol{\tau} := (\tau_{ij})$ and $\boldsymbol{\zeta} := (\zeta_{ij}) \in \mathbb{R}^{2 \times 2}$, we denote $\boldsymbol{\tau}^t := (\tau_{ji})$, $\text{tr}(\boldsymbol{\tau}) := \tau_{11} + \tau_{22}$ and $\boldsymbol{\tau} : \boldsymbol{\zeta} := \sum_{i,j=1}^2 \tau_{ij} \zeta_{ij}$. We also use the standard notations for Sobolev spaces and norms. Finally, C or c (with or without subscripts) denote generic constants, independent of the discretization parameters, that may take different values at different occurrences.

2 The dual mixed formulation

We begin this work introducing the dual mixed formulation for the Stokes system. To this end, we first reformulate problem (1) introducing the pseudostress $\boldsymbol{\sigma} := \nu \nabla \mathbf{u} - p \mathbf{I}$ in Ω as an additional unknown. Considering the compressibility condition $\operatorname{div}(\mathbf{u}) = \tilde{f}$ in Ω , it is not difficult to see that $p = \frac{\nu}{2} \tilde{f} - \frac{1}{2} \operatorname{tr}(\boldsymbol{\sigma})$ in Ω , which implies that $\boldsymbol{\sigma} \in H_0 := \{\boldsymbol{\tau} \in H(\operatorname{div}; \Omega) : \int_{\Omega} \operatorname{tr}(\boldsymbol{\tau}) = 0\}$. This relation allows us to eliminate the pressure of the second order problem (1) and thus derive the following first order system: *Find* $(\boldsymbol{\sigma}, \mathbf{u}) \in H_0 \times [H^1(\Omega)]^2$

$$\frac{1}{\nu} \boldsymbol{\sigma}^d - \nabla \mathbf{u} = -\frac{1}{2} \tilde{f} \mathbf{I} \quad \text{in } \Omega, \quad \operatorname{div}(\boldsymbol{\sigma}) = -\mathbf{f} \quad \text{in } \Omega, \quad \text{and } \mathbf{u} = \mathbf{g} \quad \text{on } \Gamma. \quad (2)$$

Proceeding in the usual way, we deduce the variational formulation based on velocity-pseudostress, which reads as follow: *Find* $(\boldsymbol{\sigma}, \mathbf{u}) \in H_0 \times [L^2(\Omega)]^2$ such that

$$\begin{aligned} a(\boldsymbol{\sigma}, \boldsymbol{\tau}) + b(\boldsymbol{\tau}, \mathbf{u}) &= G(\boldsymbol{\tau}) \quad \forall \boldsymbol{\tau} \in H_0, \\ b(\boldsymbol{\sigma}, \mathbf{v}) &= F(\mathbf{v}) \quad \forall \mathbf{v} \in [L^2(\Omega)]^2, \end{aligned} \quad (3)$$

where the bilinear forms $a : H \times H \rightarrow \mathbb{R}$ and $b : H \times [L^2(\Omega)]^2 \rightarrow \mathbb{R}$ are defined by

$$a(\boldsymbol{\sigma}, \boldsymbol{\tau}) := \frac{1}{\nu} \int_{\Omega} \boldsymbol{\sigma}^d : \boldsymbol{\tau}^d \quad \forall \boldsymbol{\sigma}, \boldsymbol{\tau} \in H \quad \text{and} \quad b(\boldsymbol{\tau}, \mathbf{v}) := \int_{\Omega} \mathbf{v} \cdot \operatorname{div}(\boldsymbol{\tau}) \quad \forall (\boldsymbol{\tau}, \mathbf{v}) \in H \times [L^2(\Omega)]^2,$$

and the linear functionals $G : H \rightarrow \mathbb{R}$ and $F : [L^2(\Omega)]^2 \rightarrow \mathbb{R}$ are given by

$$G(\boldsymbol{\tau}) := \langle \boldsymbol{\tau} \mathbf{n}, \mathbf{g} \rangle - \frac{1}{2} \int_{\Omega} \tilde{f} \operatorname{tr}(\boldsymbol{\tau}) \quad \forall \boldsymbol{\tau} \in H \quad \text{and} \quad F(\mathbf{v}) := - \int_{\Omega} \mathbf{f} \cdot \mathbf{v} \quad \forall \mathbf{v} \in [L^2(\Omega)]^2.$$

For simplicity, we introduce the spaces $\mathbf{H} := H \times [L^2(\Omega)]^2$ and $\mathbf{H}_0 := H_0 \times [L^2(\Omega)]^2$. Existence, uniqueness and stability are collected in the next result, whose proof is similar to the one of Theorem 2.1 in [7].

Theorem 1 *Problem (3) has a unique solution $(\boldsymbol{\sigma}, \mathbf{u}) \in \mathbf{H}_0$. Moreover, there exists a constant $C > 0$, independent of the solution, such that*

$$\|(\boldsymbol{\sigma}, \mathbf{u})\|_{\mathbf{H}} \leq C \left(\|\mathbf{f}\|_{[L^2(\Omega)]^2} + \|\tilde{f}\|_{L^2(\Omega)} + \|\mathbf{g}\|_{[H^{1/2}(\Gamma)]^2} \right). \quad (4)$$

2.1 An a priori error analysis

Since the dual mixed variational formulation (3) has a similar structure as the one applied for incompressible fluid flow developed in [15], in this section we establish the results for their stable pairs. In what follows, we assume that Ω is a polygonal region and let $\{\mathcal{T}_h\}_{h>0}$ be a regular family of triangulations of $\bar{\Omega}$ such that $\bar{\Omega} = \cup \{T : T \in \mathcal{T}_h\}$. Given a triangle $T \in \mathcal{T}_h$, we denote by h_T its diameter and define the mesh size $h := \max\{h_T : T \in \mathcal{T}_h\}$. In addition, given an integer $\ell \geq 0$ and

a subset S of \mathbb{R}^2 , we denote by $\mathcal{P}_\ell(S)$ the space of polynomials in two variables defined in S of total degree at most ℓ , and for each $T \in \mathcal{T}_h$, we define the local Raviart-Thomas space of order κ (cf. [23]), $\mathcal{RT}_\kappa(T) := [\mathcal{P}_\kappa(T)]^2 \oplus \mathbf{x}\mathcal{P}_\kappa(T) \subseteq [\mathcal{P}_{\kappa+1}(T)]^2 \quad \forall \mathbf{x} \in T$. Then, given an integer $r \geq 0$, we define the finite element subspaces

$$H_h^\sigma := \{ \boldsymbol{\tau}_h \in H(\mathbf{div}; \Omega) : \boldsymbol{\tau}_h|_T \in [\mathcal{RT}_r(T)]^2, \quad \forall T \in \mathcal{T}_h \},$$

$$H_{0,h}^\sigma := \left\{ \boldsymbol{\tau}_h \in H_h^\sigma : \int_\Omega \text{tr}(\boldsymbol{\tau}_h) = 0 \right\},$$

$$H_h^\mathbf{u} := \{ \mathbf{v}_h \in [L(\Omega)]^2 : \mathbf{v}_h|_T \in [\mathcal{P}_r(T)]^2, \quad \forall T \in \mathcal{T}_h \},$$

Now, setting $\mathbf{H}_{0,h} := H_{0,h}^\sigma \times H_h^\mathbf{u}$, the discrete scheme associated to variational formulation (3) reads as follows: *Find $(\boldsymbol{\sigma}_h, \mathbf{u}_h) \in \mathbf{H}_{0,h}$ such that*

$$\begin{aligned} a(\boldsymbol{\sigma}_h, \boldsymbol{\tau}) + b(\boldsymbol{\tau}, \mathbf{u}_h) &= G(\boldsymbol{\tau}) \quad \forall \boldsymbol{\tau} \in H_{0,h}^\sigma, \\ b(\boldsymbol{\sigma}_h, \mathbf{v}) &= F(\mathbf{v}) \quad \forall \mathbf{v} \in H_h^\mathbf{u}, \end{aligned} \tag{5}$$

The well posedness of this Galerkin scheme is guaranteed thanks to Babuška-Brezzi theory, and it is established in Section III in [15]. The corresponding rate of convergence of the method for this particular choice of finite element subspaces, is recalled in the next theorem.

Theorem 2 *Let $(\boldsymbol{\sigma}, \mathbf{u}) \in \mathbf{H}_0$ and $(\boldsymbol{\sigma}_h, \mathbf{u}_h) \in \mathbf{H}_{0,h}$ be the unique solutions to problems (3) and (5), respectively. In addition, Assume that $\boldsymbol{\sigma} \in [H^t(\Omega)]^{2 \times 2}$, $\mathbf{div}(\boldsymbol{\sigma}) \in [H^t(\Omega)]^2$, $\mathbf{u} \in [H^{t+1}(\Omega)]^2$ and for some $t \in (0, 1]$. Then, there exists $C > 0$, independent of h , such that there holds*

$$\begin{aligned} &\|(\boldsymbol{\sigma}, \mathbf{u}) - (\boldsymbol{\sigma}_h, \mathbf{u}_h)\|_{\mathbf{H}} \\ &\leq C h^t \left(\|\boldsymbol{\sigma}\|_{[H^t(\Omega)]^{2 \times 2}} + \|\mathbf{div}(\boldsymbol{\sigma})\|_{[H^t(\Omega)]^2} + \|\mathbf{u}\|_{[H^{t+1}(\Omega)]^2} \right). \end{aligned}$$

Proof. It is consequence of approximation properties of finite elements and Céa estimate. We omit further details. \square

3 The stabilised mixed finite element method

The aim of this section is to enlarge the set of stable pairs that allow us to approximate the solution of (3). This is obtained by modifying the bilinear form, and includes the least squares type terms

$$\delta_1 \int_\Omega (\nu \nabla \mathbf{u} - \boldsymbol{\sigma}^d) : (\boldsymbol{\tau}^d + \nu \nabla \mathbf{v}) = \frac{\delta_1 \nu^2}{2} \int_\Omega \tilde{f} \text{div}(\mathbf{v}), \quad \forall (\boldsymbol{\tau}, \mathbf{v}) \in \mathbf{H}, \tag{6}$$

$$\int_\Omega \mathbf{div}(\boldsymbol{\sigma}) \cdot \mathbf{div}(\boldsymbol{\tau}) = - \int_\Omega \mathbf{div}(\boldsymbol{\tau}) \cdot \mathbf{f} \quad \forall \boldsymbol{\tau} \in H(\mathbf{div}; \Omega), \tag{7}$$

and

$$\int_{\Gamma} \mathbf{u} \cdot \mathbf{v} = \int_{\Gamma} \mathbf{g} \cdot \mathbf{v} \quad \forall \mathbf{v} \in [H^1(\Omega)]^2. \quad (8)$$

where δ_1 is a real parameter to be determined. We denote by $\Sigma := H \times [H^1(\Omega)]^2$ and $\Sigma_0 := H_0 \times [H^1(\Omega)]^2$. Hence, we subtract the second from the first equation in (3) and then we add the terms (6), (7) and (8) to deduce the stabilised mixed formulation: *Find* $(\boldsymbol{\sigma}, \mathbf{u}) \in \Sigma_0$ *such that*

$$A((\boldsymbol{\sigma}, \mathbf{u}), (\boldsymbol{\tau}, \mathbf{v})) = \tilde{G}(\boldsymbol{\tau}, \mathbf{v}) \quad \forall (\boldsymbol{\tau}, \mathbf{v}) \in \Sigma_0, \quad (9)$$

where the bilinear form $A : \Sigma \times \Sigma \rightarrow \mathbb{R}$ and the linear functional $\tilde{G} : \Sigma \rightarrow \mathbb{R}$ are defined by

$$\begin{aligned} A((\boldsymbol{\sigma}, \mathbf{u}), (\boldsymbol{\tau}, \mathbf{v})) &:= \frac{1}{\nu} \int_{\Omega} \boldsymbol{\sigma}^d : \boldsymbol{\tau}^d + \int_{\Omega} \mathbf{u} \cdot \mathbf{div}(\boldsymbol{\tau}) - \int_{\Omega} \mathbf{v} \cdot \mathbf{div}(\boldsymbol{\sigma}) \\ &+ \delta_1 \int_{\Omega} (\nu \nabla \mathbf{u} - \boldsymbol{\sigma}^d) : (\nu \nabla \mathbf{v} + \boldsymbol{\tau}^d) + \int_{\Omega} \mathbf{div}(\boldsymbol{\sigma}) \cdot \mathbf{div}(\boldsymbol{\tau}) + \int_{\Gamma} \mathbf{u} \cdot \mathbf{v}, \end{aligned} \quad (10)$$

and

$$\begin{aligned} \tilde{G}(\boldsymbol{\tau}, \mathbf{v}) &:= \langle \boldsymbol{\tau} \mathbf{n}, \mathbf{g} \rangle - \frac{1}{2} \int_{\Omega} \tilde{f} \operatorname{tr}(\boldsymbol{\tau}) + \int_{\Omega} \mathbf{f} \cdot \mathbf{v} + \frac{\nu^2 \delta_1}{2} \int_{\Omega} \tilde{f} \operatorname{div}(\mathbf{v}) \\ &- \int_{\Omega} \mathbf{div}(\boldsymbol{\tau}) \cdot \mathbf{f} + \int_{\Gamma} \mathbf{g} \cdot \mathbf{v} \end{aligned} \quad (11)$$

Now, Proposition IV.3.1 in [13] and Lemma 3.3 in [19] allow us to establish the coercivity of the bilinear form A , which is included in the next lemma.

Lemma 3 *Let* $\delta_1 \in \mathbb{R}$ *such that* $0 < \delta_1 < \frac{1}{\nu}$. *Then, there exists a constant* $\alpha > 0$, *such that*

$$A((\boldsymbol{\tau}, \mathbf{v}), (\boldsymbol{\tau}, \mathbf{v})) \geq \alpha \|(\boldsymbol{\tau}, \mathbf{v})\|_{\Sigma}^2, \quad (12)$$

for all $(\boldsymbol{\tau}, \mathbf{v}) \in \Sigma_0$.

Furthermore, the continuity follows from straightforward application of Cauchy-Schwarz inequality. Then, existence and uniqueness of solution of Problem (9) is guaranteed thanks to Lax – Milgram’s Lemma. In addition, there exists $C > 0$, independent of the mesh size, such that

$$\|(\boldsymbol{\sigma}, \mathbf{u})\|_{\Sigma} \leq C \{ \|\mathbf{f}\|_{[L^2(\Omega)]^2} + \|\tilde{f}\|_{L^2(\Omega)} + \|\mathbf{g}\|_{[H^{1/2}(\Gamma)]^2} \} \quad (13)$$

Now, given a finite element subspace $\Sigma_{0,h} \subset \Sigma_0$, the Galerkin scheme associated with (9) reads: *Find* $(\boldsymbol{\sigma}_h, \mathbf{u}_h) \in \Sigma_{0,h}$ *such that*

$$A((\boldsymbol{\sigma}_h, \mathbf{u}_h), (\boldsymbol{\tau}, \mathbf{v})) = \tilde{G}(\boldsymbol{\tau}, \mathbf{v}) \quad \forall (\boldsymbol{\tau}, \mathbf{v}) \in \Sigma_{0,h}. \quad (14)$$

Since A is bounded and coercive on the whole space Σ_0 , we remark that the well posedness of (14) is guaranteed for any arbitrary choice of $\Sigma_{0,h}$ (a subspace of Σ_0). In fact, there exists a constant $C > 0$, independent of h , such that

$$\|(\boldsymbol{\sigma} - \boldsymbol{\sigma}_h, \mathbf{u} - \mathbf{u}_h)\|_{\Sigma} \leq C \inf_{(\boldsymbol{\tau}, \mathbf{v}) \in \Sigma_{0,h}} \|(\boldsymbol{\sigma} - \boldsymbol{\tau}, \mathbf{u} - \mathbf{v})\|_{\Sigma}. \quad (15)$$

Additionally, we note the following orthogonality relation

$$A((\boldsymbol{\sigma} - \boldsymbol{\sigma}_h, \mathbf{u} - \mathbf{u}_h), (\boldsymbol{\tau}, \mathbf{v})) = 0, \quad \forall (\boldsymbol{\tau}, \mathbf{v}) \in \boldsymbol{\Sigma}_{0,h}. \quad (16)$$

Now, in order to establish a rate of convergence result, let $m \geq 1$ and we define

$$X_h := \left\{ v_h \in \mathcal{C}(\overline{\Omega}) : v_h|_T \in \mathcal{P}_m(T), \quad \forall T \in \mathcal{T}_h \right\} \quad \text{and} \quad \mathbf{M}_h := X_h \times X_h. \quad (17)$$

Then, we consider specific finite element subspaces $\boldsymbol{\Sigma}_{0,h} := H_{0,h}^{\boldsymbol{\sigma}} \times \mathbf{M}_h$. The corresponding a priori error estimate is given in the next theorem.

Theorem 4 *Assume $\boldsymbol{\sigma} \in [H^t(\Omega)]^{2 \times 2}$, $\text{div}(\boldsymbol{\sigma}) \in [H^t(\Omega)]^2$ and $\mathbf{u} \in [H^{t+1}(\Omega)]^2$. Then, there exists $C_{\text{err}} > 0$, independent of h , such that*

$$\|(\boldsymbol{\sigma} - \boldsymbol{\sigma}_h, \mathbf{u} - \mathbf{u}_h)\|_{\boldsymbol{\Sigma}} \leq C_{\text{err}} h^{\min\{t,m,r+1\}} \left(\|\boldsymbol{\sigma}\|_{[H^t(\Omega)]^{2 \times 2}} + \|\text{div}(\boldsymbol{\sigma})\|_{[H^t(\Omega)]^2} + \|\mathbf{u}\|_{[H^{t+1}(\Omega)]^2} \right). \quad (18)$$

Proof. It follows straightforwardly from inequality (15) and the approximation properties of the corresponding finite element subspaces. We omit further details. \square

4 An a posteriori error analysis

In this section, we follow [3] (see also [11]) and develop an a posteriori error analysis for the discrete scheme (14) using an appropriate Ritz projection of the error and a quasi Helmholtz decomposition. We first introduce some notations and results concerning the Clément and Raviart-Thomas interpolation operators.

4.1 Notation and some useful results

Given $T \in \mathcal{T}_h$, we let $E(T)$ be the set of its edges, and let E_h be the set of all edges induced by the triangulation \mathcal{T}_h . Then, we write $E_h = E_I \cup E_\Gamma$, where $E_I := \{e \in E_h : e \subseteq \Omega\}$ and $E_\Gamma := \{e \in E_h : e \subseteq \Gamma\}$. Also, for each edge $e \in E_h$, we fix a unit normal vector $\mathbf{n}_e := (n_1, n_2)^\mathbf{t}$, and let $\mathbf{t}_e := (-n_2, n_1)^\mathbf{t}$ be the corresponding fixed unit tangential vector along e . From now on, when no confusion arises, we simply write \mathbf{n} and \mathbf{t} instead of \mathbf{n}_e and \mathbf{t}_e , respectively. Finally, given a smooth vector valued field $\mathbf{v} := (v_1, v_2)^\mathbf{t}$, we define

$$\underline{\text{curl}}(\mathbf{v}) := \begin{pmatrix} \frac{\partial v_1}{\partial x_2} & -\frac{\partial v_1}{\partial x_1} \\ \frac{\partial v_2}{\partial x_2} & -\frac{\partial v_2}{\partial x_1} \end{pmatrix}.$$

We will use the Clément interpolation operator $I_h : H^1(\Omega) \rightarrow X_h$ (cf. [18]), where X_h is defined in (17). A vector version of I_h , say $\mathbf{I}_h : [H^1(\Omega)]^2 \rightarrow H_h^{\mathbf{u}}$, which is defined componentwise by I_h , is also required. The following lemma establishes the local approximation properties of I_h .

Lemma 5 *There exist constants $c_1, c_2 > 0$, independent of h , such that for all $v \in H^1(\Omega)$ there holds*

$$\|v - I_h(v)\|_{H^m(T)} \leq c_1 h_T^{1-m} \|v\|_{H^1(\omega(T))}, \quad \forall m \in \{0, 1\}, \forall T \in \mathcal{T}_h,$$

and

$$\|v - I_h(v)\|_{L^2(e)} \leq c_2 h_e^{1/2} \|v\|_{H^1(\omega(e))} \quad \forall e \in E_h,$$

where $\omega(T) := \cup\{T' \in \mathcal{T}_h : T' \cap T \neq \emptyset\}$, h_e denotes the length of the side $e \in E_h$ and $\omega(e) := \cup\{T' \in \mathcal{T}_h : T' \cap e \neq \emptyset\}$.

Proof. We refer to [18]. □

On the other hand, we also need to introduce the Raviart-Thomas interpolation operator (see [13, 23]), $\Pi_h^k : [H^1(\Omega)]^{2 \times 2} \rightarrow H_h^\sigma$, which given $\boldsymbol{\tau} \in [H^1(\Omega)]^{2 \times 2}$, is characterized by the following identities:

$$\int_e \Pi_h^k(\boldsymbol{\tau}) \mathbf{n} \cdot \mathbf{q} = \int_e \boldsymbol{\tau} \mathbf{n} \cdot \mathbf{q}, \quad \forall e \in E_h, \quad \forall \mathbf{q} \in [\mathcal{P}_k(e)]^2, \quad \text{when } k \geq 0, \quad (19)$$

and

$$\int_T \Pi_h^k(\boldsymbol{\tau}) : \boldsymbol{\rho} = \int_T \boldsymbol{\tau} : \boldsymbol{\rho}, \quad \forall T \in \mathcal{T}_h, \quad \forall \boldsymbol{\rho} \in [\mathcal{P}_{k-1}(T)]^{2 \times 2}, \quad \text{when } k \geq 1. \quad (20)$$

The operator Π_h^k satisfies the following approximation properties.

Lemma 6 *There exist constants $c_3, c_4, c_5 > 0$, independent of h , such that for all $T \in \mathcal{T}_h$*

$$\|\boldsymbol{\tau} - \Pi_h^k(\boldsymbol{\tau})\|_{[L^2(T)]^{2 \times 2}} \leq c_3 h_T^m |\boldsymbol{\tau}|_{[H^m(T)]^{2 \times 2}} \quad \forall \boldsymbol{\tau} \in [H^m(\Omega)]^{2 \times 2}, \quad 1 \leq m \leq k+1 \quad (21)$$

and for all $\boldsymbol{\tau} \in [H^{m+1}(\Omega)]^{2 \times 2}$ with $\mathbf{div}(\boldsymbol{\tau}) \in [H^m(\Omega)]^2$,

$$\|\mathbf{div}(\boldsymbol{\tau} - \Pi_h^k(\boldsymbol{\tau}))\|_{[L^2(T)]^2} \leq c_4 h_T^m |\mathbf{div}(\boldsymbol{\tau})|_{[H^m(T)]^2}, \quad 0 \leq m \leq k+1 \quad (22)$$

and

$$\|\boldsymbol{\tau} \mathbf{n} - \Pi_h^k(\boldsymbol{\tau}) \mathbf{n}\|_{[L^2(e)]^2} \leq c_5 h_e^{1/2} \|\boldsymbol{\tau}\|_{[H^1(T_e)]^{2 \times 2}} \quad \forall e \in E_h, \quad \forall \boldsymbol{\tau} \in [H^1(\Omega)]^{2 \times 2}, \quad (23)$$

where $T_e \in \mathcal{T}_h$ contains e on its boundary.

Proof. See e.g. [13] or [23]. □

Moreover, the interpolation operator Π_h^k can also be defined as a bounded linear operator from the larger space $[H^s(\Omega)]^{2 \times 2} \cap H(\mathbf{div}; \Omega)$ into H_h^σ , for all $s \in (0, 1]$ (see, e.g. Theorem 3.16 in [21]). In this case, there holds the following interpolation error estimate

$$\|\boldsymbol{\tau} - \Pi_h^k(\boldsymbol{\tau})\|_{[L^2(T)]^{2 \times 2}} \leq C h_T^s \left\{ \|\boldsymbol{\tau}\|_{[H^s(T)]^{2 \times 2}} + \|\mathbf{div}(\boldsymbol{\tau})\|_{[L^2(T)]^2} \right\}, \quad \forall T \in \mathcal{T}_h.$$

Using (19) and (20), it is easy to show that

$$\mathbf{div}(\Pi_h^k(\boldsymbol{\tau})) = P_h^k(\mathbf{div}(\boldsymbol{\tau})), \quad (24)$$

where $P_h^k : [L^2(\Omega)]^2 \rightarrow H_h^u$ is the L^2 -orthogonal projector. It is well known (see, e.g. [17]) that for each $\mathbf{v} \in [H^m(\Omega)]^2$, with $0 \leq m \leq k+1$, there holds

$$\|\mathbf{v} - P_h^k(\mathbf{v})\|_{[L^2(T)]^2} \leq C h_T^m |\mathbf{v}|_{[H^m(T)]^2}, \quad \forall T \in \mathcal{T}_h. \quad (25)$$

The following inverse inequality will also be used.

Lemma 7 *Let $l, m \in \mathbb{N} \cup \{0\}$ such that $l \leq m$. Then, there exists $c > 0$, depending only on k, l, m and the shape regularity of the triangulations, such that for each $T \in \mathcal{T}_h$ there holds*

$$|q|_{H^m(T)} \leq c h_T^{l-m} |q|_{H^l(T)}, \quad \forall q \in \mathcal{P}_k(T).$$

Proof. See Theorem 3.2.6 in [17]. □

4.2 Reliability of the estimator

Let $(\boldsymbol{\sigma}, \mathbf{u})$ be the unique solution to problem (3) and assume that the Galerkin scheme (14) has a unique solution, $(\boldsymbol{\sigma}_h, \mathbf{u}_h)$. We define the Ritz projection of the error with respect to the inner product of $\boldsymbol{\Sigma}$,

$$\langle (\boldsymbol{\sigma}, \mathbf{u}), (\boldsymbol{\tau}, \mathbf{v}) \rangle_{\boldsymbol{\Sigma}} := (\boldsymbol{\sigma}, \boldsymbol{\tau})_{H(\mathbf{div}; \Omega)} + (\mathbf{u}, \mathbf{v})_{[H^1(\Omega)]^2},$$

as the unique element $(\bar{\boldsymbol{\sigma}}, \bar{\mathbf{u}}) \in \boldsymbol{\Sigma}$ such that for all $(\boldsymbol{\tau}, \mathbf{v}) \in \boldsymbol{\Sigma}$,

$$\langle (\bar{\boldsymbol{\sigma}}, \bar{\mathbf{u}}), (\boldsymbol{\tau}, \mathbf{v}) \rangle_{\boldsymbol{\Sigma}} = A((\boldsymbol{\sigma} - \boldsymbol{\sigma}_h, \mathbf{u} - \mathbf{u}_h), (\boldsymbol{\tau}, \mathbf{v})). \quad (26)$$

We remark that the existence and uniqueness of $(\bar{\boldsymbol{\sigma}}, \bar{\mathbf{u}}) \in \boldsymbol{\Sigma}$ is guaranteed by the Lax-Milgram Lemma.

Then, taking into account the coercivity of the bilinear form $A(\cdot, \cdot)$, we are able to bound the error in terms of the solution of its Ritz projection:

$$\begin{aligned} \alpha \|(\boldsymbol{\sigma} - \boldsymbol{\sigma}_h, \mathbf{u} - \mathbf{u}_h)\|_{\boldsymbol{\Sigma}} &\leq \sup_{(\boldsymbol{\tau}, \mathbf{v}) \in \boldsymbol{\Sigma}_0} \frac{A((\boldsymbol{\sigma} - \boldsymbol{\sigma}_h, \mathbf{u} - \mathbf{u}_h), (\boldsymbol{\tau}, \mathbf{v}))}{\|(\boldsymbol{\tau}, \mathbf{v})\|_{\boldsymbol{\Sigma}}} \\ &\leq \sup_{(\boldsymbol{\tau}, \mathbf{v}) \in \boldsymbol{\Sigma}} \frac{A((\boldsymbol{\sigma} - \boldsymbol{\sigma}_h, \mathbf{u} - \mathbf{u}_h), (\boldsymbol{\tau}, \mathbf{v}))}{\|(\boldsymbol{\tau}, \mathbf{v})\|_{\boldsymbol{\Sigma}}} \leq \|(\bar{\boldsymbol{\sigma}}, \bar{\mathbf{u}})\|_{\boldsymbol{\Sigma}} \end{aligned} \quad (27)$$

Then, according to (27), in order to obtain reliable a posteriori error estimates for the discrete scheme (14), it is enough to bound from above the Ritz projection of the error. To this aim, for each $\boldsymbol{\tau} \in H(\mathbf{div}; \Omega)$, we consider its quasi Helmholtz decomposition (see Lemma 5.1 in [16])

$$\boldsymbol{\tau} = \underline{\mathbf{curl}}(\boldsymbol{\chi}) + \boldsymbol{\Phi},$$

where $\boldsymbol{\chi} \in [H^1(\Omega)]^2$ and $\boldsymbol{\Phi} \in [H^1(\Omega)]^{2 \times 2}$ satisfy $\mathbf{div}(\boldsymbol{\Phi}) = \mathbf{div}(\boldsymbol{\tau})$ in Ω , and

$$\|\boldsymbol{\chi}\|_{[H^1(\Omega)]^2} + \|\boldsymbol{\Phi}\|_{[H^1(\Omega)]^{2 \times 2}} \leq C \|\boldsymbol{\tau}\|_{H(\mathbf{div}; \Omega)}.$$

Then, we let $\boldsymbol{\chi}_h := \mathbf{I}_h(\boldsymbol{\chi})$ and define

$$\boldsymbol{\tau}_h := \underline{\mathbf{curl}}(\boldsymbol{\chi}_h) + \Pi_h^k(\boldsymbol{\Phi}) \in H_h^\sigma. \quad (28)$$

We refer to (28) as a *discrete quasi Helmholtz decomposition* of $\boldsymbol{\tau}_h$. Therefore, we can write

$$\boldsymbol{\tau} - \boldsymbol{\tau}_h = \underline{\mathbf{curl}}(\boldsymbol{\chi} - \boldsymbol{\chi}_h) + \boldsymbol{\Phi} - \Pi_h^k(\boldsymbol{\Phi}), \quad (29)$$

which, using (24) and that $\mathbf{div}(\Phi) = \mathbf{div}(\tau)$ in Ω , yields

$$\mathbf{div}(\tau - \tau_h) = \mathbf{div}(\Phi - \Pi_h^k(\Phi)) = (I - P_h^k)(\mathbf{div}(\Phi)) = (I - P_h^k)(\mathbf{div}(\tau)). \quad (30)$$

On the other hand, for each $\tilde{\lambda} \in \mathbb{R}$, we note that $A((\sigma - \sigma_h, \mathbf{u} - \mathbf{u}_h), (\tilde{\lambda}\mathbf{I}, 0)) = 0$, since each $\zeta_h \in H_h^\sigma$ can be decompose as $\zeta_h = \zeta_{0,h} + \lambda\mathbf{I}$, with $\zeta_{0,h} \in H_{0,h}^\sigma$ and $\lambda \in \mathbb{R}$. The orthogonality relation (16) can be expand to

$$A((\sigma - \sigma_h, \mathbf{u} - \mathbf{u}_h), (\zeta_h, \mathbf{v}_h)) = 0, \quad \forall (\zeta_h, \mathbf{v}_h) \in \Sigma_h. \quad (31)$$

This latter remark will be useful in the next lemma, which establishes an upper bound for $\|(\bar{\sigma}, \bar{\mathbf{u}})\|_\Sigma$ in terms of residuals.

Lemma 8 *Under the assumption that $\mathbf{g} \in H^1(\Gamma)$, there exists a constant $C > 0$, independent of h , such that*

$$C \|(\bar{\sigma}, \bar{\mathbf{u}})\|_\Sigma \leq \eta := \left(\sum_{T \in \mathcal{T}_h} \eta_T^2 \right)^{1/2}, \quad (32)$$

where

$$\begin{aligned} \eta_T^2 := & \| \mathbf{f} + \mathbf{div}(\sigma_h) \|_{[L^2(T)]^2}^2 + \left\| \nabla \mathbf{u}_h - \frac{1}{\nu} \sigma_h^d - \frac{1}{2} \tilde{f} \mathbf{I} \right\|_{[L^2(T)]^{2 \times 2}}^2 + \nu^2 \delta_1^2 \| \mathbf{div}(\mathbf{u}_h) - \tilde{f} \|_{L^2(T)}^2 \\ & + \sum_{e \in E_T \cap \partial T} \left\{ h_e \| \mathbf{g} - \mathbf{u}_h \|_{[L^2(e)]^2}^2 + h_e \left\| \frac{d\mathbf{g}}{dt} - \frac{d\mathbf{u}_h}{dt} \right\|_{[L^2(e)]^2}^2 \right\}. \end{aligned}$$

Proof. First, for each $(\tau, \mathbf{v}) \in \Sigma$, we denote its induced discrete pair by $(\tau_h, \mathbf{I}_h(\mathbf{v})) \in \Sigma_h$, where τ_h is defined in (28) and $\mathbf{I}_h(\mathbf{v})$ is the Clément interpolant of \mathbf{v} . Hence, We use (31) with $(\zeta_h, \mathbf{v}_h) = (\tau_h, \mathbf{I}_h(\mathbf{v}))$ and that (σ, \mathbf{u}) is the unique solution for Problem (9) to obtain

$$\begin{aligned} \langle (\bar{\sigma}, \bar{\mathbf{u}}), (\tau, \mathbf{v}) \rangle_\Sigma &= A((\sigma - \sigma_h, \mathbf{u} - \mathbf{u}_h), (\tau - \tau_h, \mathbf{v} - \mathbf{I}_h(\mathbf{v}))) \\ &= \tilde{G}(\tau - \tau_h, \mathbf{v} - \mathbf{I}_h(\mathbf{v})) - A((\sigma_h, \mathbf{u}_h), (\tau - \tau_h, \mathbf{v} - \mathbf{I}_h(\mathbf{v}))) \end{aligned}$$

Equivalently,

$$\begin{aligned} (\bar{\sigma}, \tau)_{H(\mathbf{div}; \Omega)} &= F_1(\tau - \tau_h), \quad \forall \tau \in H(\mathbf{div}; \Omega), \\ (\bar{\mathbf{u}}, \mathbf{v})_{[H^1(\Omega)]^2} &= F_2(\mathbf{v} - \mathbf{I}_h(\mathbf{v})), \quad \forall \mathbf{v} \in [H^1(\Omega)]^2, \end{aligned}$$

where $F_1 : H(\mathbf{div}; \Omega) \rightarrow \mathbb{R}$ and $F_2 : [H^1(\Omega)]^2 \rightarrow \mathbb{R}$ are the bounded linear functionals defined as

$$\begin{aligned} F_1(\rho) := & - \int_\Omega (\mathbf{f} + \mathbf{div}(\sigma_h)) \cdot \mathbf{div}(\rho) - \int_\Omega \left(\frac{1}{\nu} \sigma_h^d - \nabla \mathbf{u}_h + \frac{1}{2} \tilde{f} \mathbf{I} \right) : (\rho) \\ & + \langle (\rho) \mathbf{n}, \mathbf{g} - \mathbf{u}_h \rangle - \delta_1 \nu \int_\Omega \left(\nabla \mathbf{u}_h - \frac{1}{\nu} \sigma_h^d - \frac{1}{2} \tilde{f} \mathbf{I} \right) : (\rho)^d \quad \forall \rho \in H(\mathbf{div}; \Omega), \end{aligned}$$

$$\begin{aligned}
F_2(\mathbf{w}) &:= \int_{\Omega} (\mathbf{f} + \mathbf{div}(\boldsymbol{\sigma}_h)) \cdot \mathbf{w} - \delta_1 \nu^2 \int_{\Omega} (\nabla \mathbf{u}_h - \frac{1}{\nu} \boldsymbol{\sigma}_h^d - \frac{1}{2} \tilde{f} \mathbf{I}) : \nabla \mathbf{w} \\
&+ \int_{\Gamma} (\mathbf{g} - \mathbf{u}_h) \cdot \mathbf{w} \quad \forall \mathbf{w} \in [H^1(\Omega)]^2.
\end{aligned}$$

Now, using (29), and then proceeding as in Lemmas 3.6, 3.7 and 3.8 in [6], we deduce that there exists $c > 0$, independent of h , such that

$$\begin{aligned}
&c|F_1(\boldsymbol{\tau} - \boldsymbol{\tau}_h)| \\
&\leq \left(\sum_{T \in \mathcal{T}_h} \left\{ \|\mathbf{div}(\boldsymbol{\sigma}_h) + \mathbf{f}\|_{[L^2(T)]^2}^2 + \|\nabla \mathbf{u}_h - \frac{1}{\nu} \boldsymbol{\sigma}_h^d - \frac{1}{2} \tilde{f} \mathbf{I}\|_{[L^2(T)]^{2 \times 2}}^2 + \nu^2 \delta_1^2 \|\mathbf{div}(\mathbf{u}_h) - \tilde{f}\|_{L^2(T)}^2 \right\} \right. \\
&\quad \left. + \sum_{e \in E_{\Gamma}} \left\{ h_e \|\mathbf{g} - \mathbf{u}_h\|_{[L^2(e)]^2}^2 + h_e \left\| \frac{d\mathbf{g}}{dt} - \frac{d\mathbf{u}_h}{dt} \right\|_{[L^2(e)]^2}^2 \right\} \right)^{1/2} \|\boldsymbol{\tau}\|_{H(\mathbf{div}; \Omega)}.
\end{aligned}$$

In the same spirit, applying Cauchy - Schwarz inequality and Lemma 5, we infer that there exists $c > 0$, independent of h , such that

$$\begin{aligned}
&c|F_2(\mathbf{v} - \mathbf{I}_h(\mathbf{v}))| \\
&\leq \left(\sum_{T \in \mathcal{T}_h} \left\{ h_T^2 \|\mathbf{div}(\boldsymbol{\sigma}_h) + \mathbf{f}\|_{[L^2(T)]^2}^2 + \delta_1^2 \nu^4 \|\nabla \mathbf{u}_h - \frac{1}{\nu} \boldsymbol{\sigma}_h^d - \frac{1}{2} \tilde{f} \mathbf{I}\|_{[L^2(T)]^{2 \times 2}}^2 \right\} \right. \\
&\quad \left. + \sum_{e \in E_{\Gamma}} h_e \|\mathbf{g} - \mathbf{u}_h\|_{[L^2(e)]^2}^2 \right)^{1/2} \|\mathbf{v}\|_{[H^1(\Omega)]^2}.
\end{aligned}$$

Hence, the proof follows from the above bounds and a discrete Cauchy - Schwarz inequality. \square

Motivated by the previous results, we define the a posteriori error estimate

$$\eta := \left(\sum_{T \in \mathcal{T}_h} \eta_T^2 \right)^{1/2},$$

where

$$\begin{aligned}
\eta_T^2 &:= \|\mathbf{f} + \mathbf{div}(\boldsymbol{\sigma}_h)\|_{[L^2(T)]^2}^2 + \left\| \nabla \mathbf{u}_h - \frac{1}{\nu} \boldsymbol{\sigma}_h^d - \frac{1}{2} \tilde{f} \mathbf{I} \right\|_{[L^2(T)]^{2 \times 2}}^2 + \nu^2 \delta_1^2 \|\mathbf{div}(\mathbf{u}_h) - \tilde{f}\|_{L^2(T)}^2 \\
&+ \sum_{e \in E_{\Gamma} \cap \partial T} \left\{ h_e \|\mathbf{g} - \mathbf{u}_h\|_{[L^2(e)]^2}^2 + h_e \left\| \frac{d\mathbf{g}}{dt} - \frac{d\mathbf{u}_h}{dt} \right\|_{[L^2(e)]^2}^2 \right\}
\end{aligned}$$

In summary, in the next result we establish that the a posteriori error estimator η is reliable and efficient.

Theorem 9 Assuming that $\mathbf{g} \in [H^1(\Gamma)]^2$, there exists a positive constant C_{rel} , independent of h , such that

$$\|(\boldsymbol{\sigma} - \boldsymbol{\sigma}_h, \mathbf{u} - \mathbf{u}_h)\|_{\Sigma} \leq C_{\text{rel}} \eta.$$

Additionally, there exists $C_{\text{eff}} > 0$, independent of h , such that

$$\eta_T^2 \leq C_{\text{eff}} \|(\boldsymbol{\sigma} - \boldsymbol{\sigma}_h, \mathbf{u} - \mathbf{u}_h)\|_T \quad (33)$$

with $\|(\boldsymbol{\tau}, \mathbf{v})\|_T^2 := \|\boldsymbol{\tau}\|_{H(\text{div}; T)}^2 + \|\mathbf{v}\|_{[H^1(T)]^2}^2$

Proof. The reliability of η (first inequality) follows from (27) and Lemma 8. The efficiency of η (second inequality) is treated in the next subsection. We omit further details. \square

4.3 Efficiency of the estimator

In this section, we proceed to establish the local efficiency of the local a posteriori error estimate (33). Since $\mathbf{f} = -\text{div}(\boldsymbol{\sigma})$ in Ω and $\frac{1}{\nu}\boldsymbol{\sigma}^d - \nabla\mathbf{u} = -\frac{1}{2}\tilde{f}\mathbf{I}$ in Ω , we have that

$$\|\mathbf{f} + \text{div}(\boldsymbol{\sigma}_h)\|_{[L^2(T)]^2} = \|\text{div}(\boldsymbol{\sigma} - \boldsymbol{\sigma}_h)\|_{[L^2(T)]^2},$$

and

$$\|\nabla\mathbf{u}_h - \frac{1}{\nu}\boldsymbol{\sigma}_h^d - \frac{1}{2}\tilde{f}\mathbf{I}\|_{[L^2(T)]^{2 \times 2}} \leq |\mathbf{u} - \mathbf{u}_h|_{[H^1(T)]^2} + \frac{(1 + \sqrt{2})}{\nu} \|\boldsymbol{\sigma} - \boldsymbol{\sigma}_h\|_{[L^2(T)]^{2 \times 2}}.$$

Furthermore, using that $\text{div}(\mathbf{u}) = \tilde{f}$ in Ω , we deduce

$$\|\text{div}(\mathbf{u}_h) - \tilde{f}\|_{L^2(T)} = \|\text{div}(\mathbf{u} - \mathbf{u}_h)\|_{L^2(T)} \leq \sqrt{2} |\mathbf{u} - \mathbf{u}_h|_{[H^1(T)]^2}.$$

Now, in order to bound the boundary terms $h_e \|\mathbf{g} - \mathbf{u}_h\|_{[L^2(e)]^2}^2$, $e \in E_\Gamma$, we need to recall a discrete trace inequality. Indeed, as established in Theorem 3.10 in [1] (see also equation (2.4) in [2]), there exists $c > 0$, depending only on the shape regularity of the triangulations, such that for each $T \in \mathcal{T}_h$ and $e \in E(T)$, there holds

$$\|v\|_{L^2(e)}^2 \leq c \left\{ h_e^{-1} \|v\|_{L^2(T)}^2 + h_e \|v\|_{H^1(T)}^2 \right\}, \quad \forall v \in H^1(T). \quad (34)$$

Lemma 10 There exists $C > 0$, independent of h , such that for each $e \in E_\Gamma$ there holds

$$h_e \|\mathbf{g} - \mathbf{u}_h\|_{[L^2(e)]^2}^2 \leq C \left(\|\mathbf{u} - \mathbf{u}_h\|_{[L^2(T_e)]^2}^2 + h_{T_e}^2 |\mathbf{u} - \mathbf{u}_h|_{[H^1(T_e)]^2}^2 \right),$$

where T_e is the triangle having e as an edge.

Proof. It is a straightforward application of (34), taking into account that $\mathbf{u} = \mathbf{g}$ on Γ . \square

The last term is studied in the following lemma.

Lemma 11 Assume $\mathbf{g} \in [H^1(\Gamma)]^2$ is component-piecewise polynomial on Γ . Then there exists $C > 0$, independent of h , such that for each $e \in E_\Gamma$ there holds

$$h_e \left\| \frac{d\mathbf{g}}{dt} - \frac{d\mathbf{u}_h}{dt} \right\|_{[L^2(e)]^2}^2 \leq C |\mathbf{u} - \mathbf{u}_h|_{[H^1(T_e)]^2}^2, \quad (35)$$

where T_e is the triangle having e as an edge.

Proof. See Lemma 3.10 in [6]. \square

5 Numerical experiments

We begin this section by remarking that, for implementation purposes, the null media condition required by the basis of $H_{0,h}^{\boldsymbol{\sigma}}$ can be circumvented by imposing this requirement through a Lagrange multiplier. More precisely, we solve the following auxiliary discrete scheme: Find $(\boldsymbol{\sigma}_h, \mathbf{u}_h, \varphi_h) \in \mathbf{H}_h := H_h^{\boldsymbol{\sigma}} \times H_h^{\mathbf{u}} \times \mathbb{R}$ such that

$$\begin{aligned} A((\boldsymbol{\sigma}_h, \mathbf{u}_h), (\boldsymbol{\tau}_h, \mathbf{v}_h)) + \varphi_h \int_{\Omega} \operatorname{tr}(\boldsymbol{\tau}_h) &= \tilde{G}(\boldsymbol{\tau}_h, \mathbf{v}_h), \\ \psi_h \int_{\Omega} \operatorname{tr}(\boldsymbol{\sigma}_h) &= 0, \end{aligned} \tag{36}$$

for all $(\boldsymbol{\tau}_h, \mathbf{v}_h, \psi_h) \in \mathbf{H}_h$. A standard argument establishes the equivalence between the variational problems (14) and (36), for details see for example Theorem 6.1 in [4].

In what follows, *DOF* stands for the total number of degrees of freedom (unknowns) of (36), that is, $DOF = 2 \times (\text{Numbers of vertexes of } \mathcal{T}_h) + 2 \times (\text{Number of edges } \mathcal{T}_h) + 1$, which leads asymptotically to 4 unknowns per triangle, which reflects the low computational cost, almost the same than the required by considering the \mathcal{P}_1 -iso \mathcal{P}_1 elements for the standard velocity-pressure formulation, whose degrees of freedom are asymptotically 4.5 (unknowns) per triangle. In addition, by setting $p_h := -\frac{1}{2}\operatorname{tr}(\boldsymbol{\sigma}_h)$, we obtain a reasonable piecewise-linear approximation of the pressure $p := -\frac{1}{2}\operatorname{tr}(\boldsymbol{\sigma})$.

Hereafter, the individual and total errors are denoted as follows

$$\begin{aligned} \mathbf{e}(\mathbf{u}) &:= \|\mathbf{u} - \mathbf{u}_h\|_{[H^1(\Omega)]^2}, \quad \mathbf{e}(\boldsymbol{\sigma}) := \|\boldsymbol{\sigma} - \boldsymbol{\sigma}_h\|_{H(\operatorname{div}, \Omega)}, \quad \mathbf{e} := \left([\mathbf{e}(\mathbf{u})]^2 + [\mathbf{e}(\boldsymbol{\sigma})]^2 \right)^{1/2}, \\ \mathbf{e}_0(p) &:= \|p + \frac{1}{2}\operatorname{tr}(\boldsymbol{\sigma}_h)\|_{L^2(\Omega)}, \quad \mathbf{e}_0(\boldsymbol{\sigma}^d) := \|\boldsymbol{\sigma}^d - \boldsymbol{\sigma}_h^d\|_{[L^2(\Omega)]^{2 \times 2}} \\ &\text{and } \mathbf{e}_0(\mathbf{u}) := \|\mathbf{u} - \mathbf{u}_h\|_{[L^2(\Omega)]^2}, \end{aligned}$$

where $(\boldsymbol{\sigma}, \mathbf{u}) \in H_0 \times [H^1(\Omega)]^2$ and $(\boldsymbol{\sigma}_h, \mathbf{u}_h) \in H_{0,h}^{\boldsymbol{\sigma}} \times H_h^{\mathbf{u}}$ are the unique solutions of the continuous and discrete formulations, respectively. In addition, if \mathbf{e} and $\tilde{\mathbf{e}}$ stand for the errors at two consecutive triangulations with N and \tilde{N} degrees of freedom, respectively, then the experimental rate of convergence is given by $r := -2 \frac{\log(\mathbf{e}/\tilde{\mathbf{e}})}{\log(N/\tilde{N})}$. The definitions of $r(\mathbf{u})$, $r(\boldsymbol{\sigma})$, $r_0(\boldsymbol{\sigma}^d)$, $r_0(\mathbf{u})$ and $r_0(p)$ are defined analogously.

5.1 Robustness of the method

The aim here is to exhibit the robustness of our scheme with respect to the viscosity parameter ν . To do this, we consider the two-dimensional analytical solution of the Navier-Stokes equations derived by Kovasznay in [22], where the velocity, the pressure and the domain are given by:

$$\mathbf{u}(x, y) = \begin{pmatrix} 1 - e^{\lambda x} \cos(2\pi y) \\ \frac{\lambda}{2\pi} e^{\lambda x} \sin(2\pi y) \end{pmatrix}, \quad p(x, y) = -\frac{1}{2} e^{2\lambda x} - p_0, \quad \Omega = (-1/2, 3/2) \times (0, 2), \tag{37}$$

with the constant p_0 is chosen to ensure $p \in L_0^2(\Omega)$ and the parameter λ is given by:

$$\lambda = -\frac{8\pi^2}{\nu^{-1} + \sqrt{\nu^{-2} + 16\pi^2}}.$$

We emphasize that here $\operatorname{div}(\mathbf{u}) = 0$ in Ω (so the fluid is incompressible) and the solution is smooth. This is the reason why we present the results just for uniform refinement, and with the viscosity ν ranging from 1 to 10^{-4} , i.e., for small values of the viscosity. This is in accordance with our interest in developing an scheme for compressible flow, which usually occurs for small values of viscosity. Tables 1, 2 and 3 show that our scheme is able to deal with moderate small values of viscosity ν . In all these cases, the method does converge to the exact solution, and with the expected optimal rate of convergence, as is exposed in Figure 1.

5.2 Testing the deduced a posteriori error estimator

In the next examples, we focus our attention in the iterative process to approximate the exact solution applying an adaptive algorithm in the mesh refinement, based on our estimator η_T . The algorithm we consider can be found in [25], and reads as follows:

1. Start with a coarse mesh \mathcal{T}_h .
2. Solve the Galerkin scheme for the current mesh \mathcal{T}_h .
3. Compute η_T for each triangle $T \in \mathcal{T}_h$.
4. Consider stopping criterion and decide to finish or go to the next step.
5. Use *Red-blue-green* procedure to refine each element $T' \in \mathcal{T}_h$ such that

$$\eta_{T'} \geq \frac{1}{2} \max\{\eta_T : T \in \mathcal{T}_h\}.$$

6. Define the resulting mesh as the new \mathcal{T}_h and go to step 2.

5.2.1 Example 2: Boundary Layer

It is very well known that Kovasznay solution (see [22]) given in Example 1, present a boundary layer for a large value of the viscosity, therefore in this example we consider this analytical solution with viscosity $\nu = 1$. The data contained in Table 4 show us that our a posteriori error estimator is capable to improve the quality of approximation of the solution, as is noticed from Figure 2. In addition, looking at the index of efficiency column, we notice that our estimator is reliable and efficient, as predicted by the theory. Figure 4 shows us that the considered adaptive algorithm is able to find the boundary layer along the segment $\{-1/2\} \times [0, 2]$.

5.2.2 Example 3: A compressible example

Here we consider the circular section $\Omega := \{(x_1, x_2) \in \mathbb{R}^2 : x_1^2 + x_2^2 < 1\} \setminus ([0, 1] \times [-1, 0])$. Then, we consider the data \mathbf{f} and \mathbf{g} are chosen so that the exact solution (\mathbf{u}, p) is given by

$$\mathbf{u}(x_1, x_2) := \frac{1}{8\pi\nu} \left\{ -\ln(s) \begin{pmatrix} 1 \\ 0 \end{pmatrix} + \frac{1}{s^2} \begin{pmatrix} (x_1 - 2)^2 \\ (x_1 - 2)(x_2 - 1) \end{pmatrix} \right\} + \begin{pmatrix} x_1^2 \\ x_2^2 \end{pmatrix},$$

and

$$p(r, \theta) := r^{2/3} \sin\left(\frac{2}{3}\theta\right) - \frac{3}{2\pi},$$

where $s := \sqrt{(x_1 - 2)^2 + (x_2 - 2)^2}$, and the pressure p is given in polar coordinates. We remark here that $\operatorname{div}(\mathbf{u}) = 2(x_1 + x_2)$, thus we are dealing with a compressible fluid. Table 5 reports us that the numerical approximation is improved by applying the proposed adaptive algorithm, based on η_T . We also observe that the index of efficiency remains close to 1, thus allowing to conclude that our estimator is reliable and efficient. Figure 5 contains a sequence of adapted meshes, based on η_T , from which we notice that the algorithm is able to detect the singularity at origin.

6 Conclusion and final comments

In this paper, we have extended the applicability of the augmented mixed finite element method to compressible fluid flow. We present the dual mixed approach as well as the corresponding stabilised mixed fomulation, based on the introduction of appropriate least squares terms. The a priori error analysis for both schemes are presented. Additionally, an a posteriori error estimador is developed for the stabilised one. It is important to mention that our a posteriori error indicator consists only of five residual terms to be computed on each triangle and it does not contain any jumps across the edges of the mesh. Moreover, it is shown to be reliable and locally efficient. Numerical results show its good performance in practice, with efficiency indices around 1 in all the tests examples. We remark that the a posteriori error indicator proposed in this paper can be easily generalized to 3D. Furthermore, when the problem is reduced to the particular case of incompressible fluid flow (i.e. when $\tilde{f} = 0$), the stabilised approach is the same as the one developed in [19], which the authors obtain an a posteriori error estimator consisting on 12 terms. In this sense, we propose in this paper an a posteriori error estimator of low computational cost for a compressible fluid flow model.

Acknowledgments. This research was partially supported by CONICYT-Chile through FONDECYT Grant 1160578, by CONICYT-Chile through project AFB170001 of the PIA Program: Concurso Apoyo a Centros Científicos y Tecnológicos de Excelencia con Financiamiento Basal, by Vicerrectoría de Investigación y Desarrollo de la Universidad de Concepción through project VRID-Enlace No. 218.013.044-1.0, by Centro de Investigación en Ingeniería Matemática (CI²MA), Universidad de Concepción (Chile), and by the Dirección de Investigación de la Universidad Católica de la Santísima Concepción, Concepción (Chile).

dof	$e(\mathbf{u})$	$r(\mathbf{u})$	$e(\boldsymbol{\sigma})$	$r(\boldsymbol{\sigma})$	e	r	e/η
291	0.575e+2	—	0.317e+3	—	0.322e+3	—	0.9745
1091	0.327e+2	0.8560	0.204e+3	0.6689	0.206e+3	0.6742	0.9928
4227	0.167e+2	0.9889	0.111e+3	0.8979	0.112e+3	0.9000	1.0014
16643	0.839e+1	1.0061	0.568e+2	0.9770	0.574e+2	0.9777	1.0049
66051	0.420e+1	1.0055	0.286e+2	0.9968	0.289e+2	0.9970	1.0066
263171	0.210e+1	1.0032	0.143e+2	1.0006	0.145e+2	1.0007	1.0074
1050627	0.105e+1	1.0016	0.716e+1	1.0009	0.723e+1	1.0009	1.0077

Table 1: History of convergence and corresponding rates of convergence, Example 1, $\nu = 1.0$ (uniform refinement)

dof	$e(\mathbf{u})$	$r(\mathbf{u})$	$e(\boldsymbol{\sigma})$	$r(\boldsymbol{\sigma})$	e	r	e/η
291	0.387e+1	—	0.314e+0	—	0.389e+1	—	0.5141
1091	0.251e+1	0.6570	0.153e+0	1.0910	0.251e+1	0.6592	0.5173
4227	0.130e+1	0.9769	0.749e-1	1.0499	0.130e+1	0.9771	0.5367
16643	0.650e+0	1.0058	0.372e-1	1.0204	0.651e+0	1.0059	0.5437
66051	0.325e+0	1.0048	0.186e-1	1.0081	0.326e+0	1.0048	0.5475
263171	0.163e+0	1.0026	0.929e-2	1.0034	0.163e+0	1.0026	0.5497
1050627	0.813e-1	1.0014	0.464e-2	1.0016	0.815e-1	1.0014	0.5509

Table 2: History of convergence and corresponding rates of convergence, Example 1, $\nu = 0.01$ (uniform refinement)

dof	$e(\mathbf{u})$	$r(\mathbf{u})$	$e(\boldsymbol{\sigma})$	$r(\boldsymbol{\sigma})$	e	r	e/η
291	0.449e+1	—	0.507e-2	—	0.449e+1	—	0.5212
1091	0.290e+1	0.6611	0.510e-2	—	0.290e+1	0.6611	0.5138
4227	0.150e+1	0.9763	0.277e-2	0.9038	0.150e+1	0.9763	0.5282
16643	0.749e+0	1.0127	0.105e-2	1.4160	0.749e+0	1.0127	0.5282
66051	0.373e+0	1.0113	0.349e-3	1.5943	0.373e+0	1.0113	0.5270
263171	0.186e+0	1.0056	0.129e-3	1.4397	0.186e+0	1.0056	0.5270
1050627	0.930e-1	1.0023	0.565e-4	1.1948	0.930e-1	1.0023	0.5275

Table 3: History of convergence and corresponding rates of convergence, Example 1, $\nu = 0.0001$ (uniform refinement)

References

- [1] S. Agmon, Lectures on Elliptic Boundary Value Problems. Van Nostrand, Princeton, New Jersey, 1965.
- [2] D.N. Arnold, *An interior penalty finite element method with discontinuous elements*. SIAM Journal on Numerical Analysis, vol. 19, 4, pp. 742-760, (1982).

dof	$e(\mathbf{u})$	$r(\mathbf{u})$	$e(\boldsymbol{\sigma})$	$r(\boldsymbol{\sigma})$	e	r	e/η
291	0.575e+2	—	0.317e+3	—	0.322e+3	—	0.9745
1091	0.327e+2	0.8560	0.204e+3	0.6689	0.206e+3	0.6742	0.9928
4227	0.167e+2	0.9889	0.111e+3	0.8979	0.112e+3	0.9000	1.0014
16643	0.839e+1	1.0061	0.568e+2	0.9770	0.574e+2	0.9777	1.0049
66051	0.420e+1	1.0055	0.286e+2	0.9968	0.289e+2	0.9970	1.0066
263171	0.210e+1	1.0032	0.143e+2	1.0006	0.145e+2	1.0007	1.0074
1050627	0.105e+1	1.0016	0.716e+1	1.0009	0.723e+1	1.0009	1.0077
dof	$e(\mathbf{u})$	$r(\mathbf{u})$	$e(\boldsymbol{\sigma})$	$r(\boldsymbol{\sigma})$	e	r	e/η
291	0.575e+2	—	0.317e+3	—	0.322e+3	—	0.9745
415	0.334e+2	3.0565	0.202e+3	2.5323	0.205e+3	2.5476	0.9930
883	0.181e+2	1.6211	0.113e+3	1.5337	0.115e+3	1.5360	1.0028
1495	0.134e+2	1.1421	0.723e+2	1.7086	0.735e+2	1.6922	1.0108
3947	0.848e+1	0.9469	0.435e+2	1.0440	0.444e+2	1.0406	1.0132
6811	0.645e+1	1.0002	0.339e+2	0.9187	0.345e+2	0.9216	1.0131
14887	0.461e+1	0.8628	0.226e+2	1.0374	0.231e+2	1.0308	1.0149
24723	0.362e+1	0.9443	0.178e+2	0.9322	0.182e+2	0.9326	1.0146
58707	0.238e+1	0.9728	0.115e+2	1.0249	0.117e+2	1.0227	1.0160
100623	0.180e+1	1.0325	0.890e+1	0.9342	0.908e+1	0.9381	1.0157
232035	0.121e+1	0.9572	0.580e+1	1.0266	0.592e+1	1.0238	1.0162
366015	0.936e+0	1.1219	0.467e+1	0.9470	0.477e+1	0.9541	1.0156
820439	0.651e+0	0.8984	0.316e+1	0.9700	0.323e+1	0.9671	1.0161

Table 4: History of convergence and corresponding rates of convergence, Example 2, $\nu = 1.0$ (uniform and adaptive refinements)

- [3] T. P. Barrios, E. M. Behrens and M. González. *Low cost A posteriori error estimators for an augmented mixed FEM in linear elasticity*. Applied Numerical Mathematics, vol. 84, pp. 46-65, (2014).
- [4] T.P. Barrios, R. Bustinza, G. C. García, and E. Hernández. *On stabilized mixed methods for generalized Stokes problem based on the velocity-pseudostress formulation: A priori error estimates*. Computer Methods in Applied Mechanics and Engineering, vol. 237-240, pp. 78-87, (2012).
- [5] T. P. Barrios, R. Bustinza, G.C. García and M. González, *An a posteriori error estimator for a new stabilized formulation of the Brinkman problem*. Numerical Mathematics and Advanced Applications - ENUMATH-2013, 10th European Conference on Numerical Mathematics and Advanced Applications, Lausanne, August 2013. Abdulle, A., Deparis, S., Kressner, D., Nobile, F., Picasso, M. (Editors), LNCSE, Vol. 103, pp. 263 - 271. Springer Verlag, 2015.
- [6] T. P. Barrios, R. Bustinza, G.C. García and M. González, *An a posteriori error analysis of a velocity-pseudostress formulation of the generalized Stokes problem*. Journal of Computational and Applied Mathematics, vol 357, 349-365, (2019).

dof	$\mathbf{e}(\mathbf{u})$	$r(\mathbf{u})$	$\mathbf{e}(\boldsymbol{\sigma})$	$r(\boldsymbol{\sigma})$	\mathbf{e}	r	\mathbf{e}/η
12819	0.484e-1	—	0.559e-1	—	0.739e-1	—	0.9566
50723	0.243e-1	1.0061	0.316e-1	0.8296	0.398e-1	0.9002	0.9772
201795	0.121e-1	1.0034	0.187e-1	0.7593	0.223e-1	0.8406	1.0086
804995	0.607e-2	1.0018	0.119e-1	0.6542	0.133e-1	0.7410	1.0826
dof	$\mathbf{e}(\mathbf{u})$	$r(\mathbf{u})$	$\mathbf{e}(\boldsymbol{\sigma})$	$r(\boldsymbol{\sigma})$	\mathbf{e}	r	\mathbf{e}/η
12819	0.484e-1	—	0.559e-1	—	0.739e-1	—	0.9566
12943	0.484e-1	0.3126	0.509e-1	19.1889	0.702e-1	10.6621	0.9526
13067	0.484e-1	0.0191	0.489e-1	8.6916	0.688e-1	4.4889	0.9507
13339	0.483e-1	0.1533	0.474e-1	2.9472	0.677e-1	1.5443	0.9497
19045	0.434e-1	0.5960	0.414e-1	0.7585	0.600e-1	0.6746	0.9615
36925	0.316e-1	0.9608	0.306e-1	0.9173	0.440e-1	0.9399	0.9693
52175	0.255e-1	1.2427	0.252e-1	1.1255	0.358e-1	1.1855	0.9688
80011	0.218e-1	0.7292	0.212e-1	0.8046	0.304e-1	0.7661	0.9772
148975	0.161e-1	0.9790	0.162e-1	0.8637	0.228e-1	0.9220	0.9962
210329	0.131e-1	1.2052	0.136e-1	0.9947	0.189e-1	1.0973	1.0089
322383	0.110e-1	0.8060	0.117e-1	0.7184	0.161e-1	0.7599	1.0281
593509	0.818e-2	0.9696	0.952e-2	0.6754	0.126e-1	0.8069	1.0824
845559	0.665e-2	1.1759	0.843e-2	0.6920	0.107e-1	0.8875	1.1345

Table 5: History of convergence and corresponding rates of convergence, Example 3, $\nu = 1.0$ (uniform and adaptive refinements)

- [7] T. P. Barrios, R. Bustinza and F. Sánchez: *Analysis of DG approximations for Stokes problem based on velocity-pseudostress formulation*. Numerical Methods for Partial Differential Equations, **vol. 33, 5**, pp. 1540-1564, (2017).
- [8] T. P. Barrios, J. M. Cascón and M. González, *A posteriori error analysis of a stabilized mixed finite element method for Darcy flow*. Computer Methods in Applied Mechanics and Engineering, **vol. 283**, pp. 909-922, (2015).
- [9] T. P. Barrios, J. M. Cascón and M. González, *A posteriori error estimation of a stabilized mixed finite element method for Darcy flow*. In book: Proceedings of International conference Boundary and Interior Layers - Computational & Asymptotic Methods, BAIL 2014 (Edited by Petr Knobloch). Springer series Lecture Notes in Computational Science and Engineering. Vol 108, pp 13 - 23. (2015).
- [10] T. P. Barrios, J. M. Cascón and M. González, *Augmented mixed finite element method for the Oseen problem: A priori and a posteriori error analysis*. Computer Methods in Applied Mechanics and Engineering, Vol. 313, pp. 216-238, (2017).
- [11] T.P. Barrios and G.N. Gatica. *An augmented mixed finite element method with Lagrange multipliers: A priori and a posteriori error analyses*. J. Comput. Appl. Math. 200, 653–676 (2007).

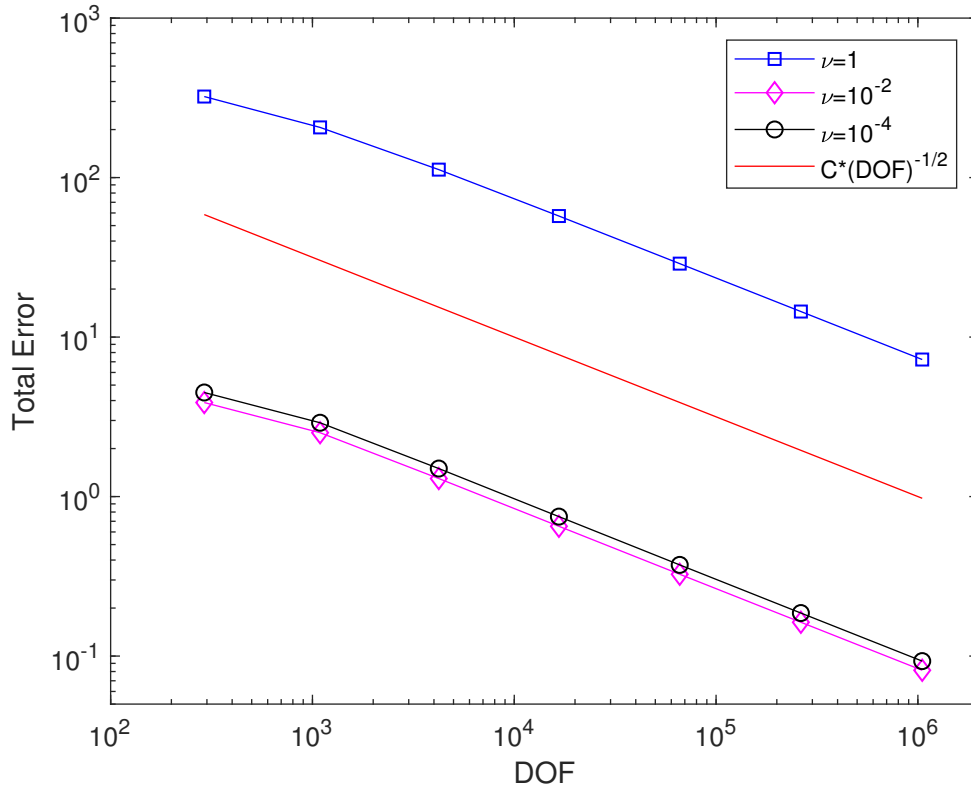


Figure 1: Total error (e) vs DOF (N) for uniform refinements (Example 1, with $\nu \in \{1, 0.01, 0.0001\}$)

- [12] T.P. Barrios, G.N. Gatica, M. González and N. Heuer. *A residual based a posteriori error estimator for an augmented mixed finite element method in linear elasticity*. M2AN Math. Model. Numer. Anal. 40, 843–869 (2006).
- [13] F. Brezzi and M. Fortin. *Mixed and hybrid finite element methods*. Springer Series in Computational Mathematics 15, Springer-Verlag, New York, 1991.
- [14] Z. Cai, B. Lee and P. Wang, *Least-squares methods for incompressible Newtonian fluid flow: Linear stationary problems*. SIAM Journal of Numerical Analysis, vol. 42, pp. 843-859, (2004).
- [15] Z. Cai, C. Tong, P.S. Vassilevski and C. Wang. *Mixed finite element methods for incompressible flow: Stationary Stokes equations*. Numerical Methods for Partial Diferential Equations, vol. 26, pp. 957-978, (2010).
- [16] J. M. Cascón, R. H. Nochetto and K. G. Siebert, *Design and Convergence of AFEM in $H(DIV)$* , Mathematical Models and Methods in Applied Sciences. vol. 17 (11), pp. 1849 - 1881 , (2007).

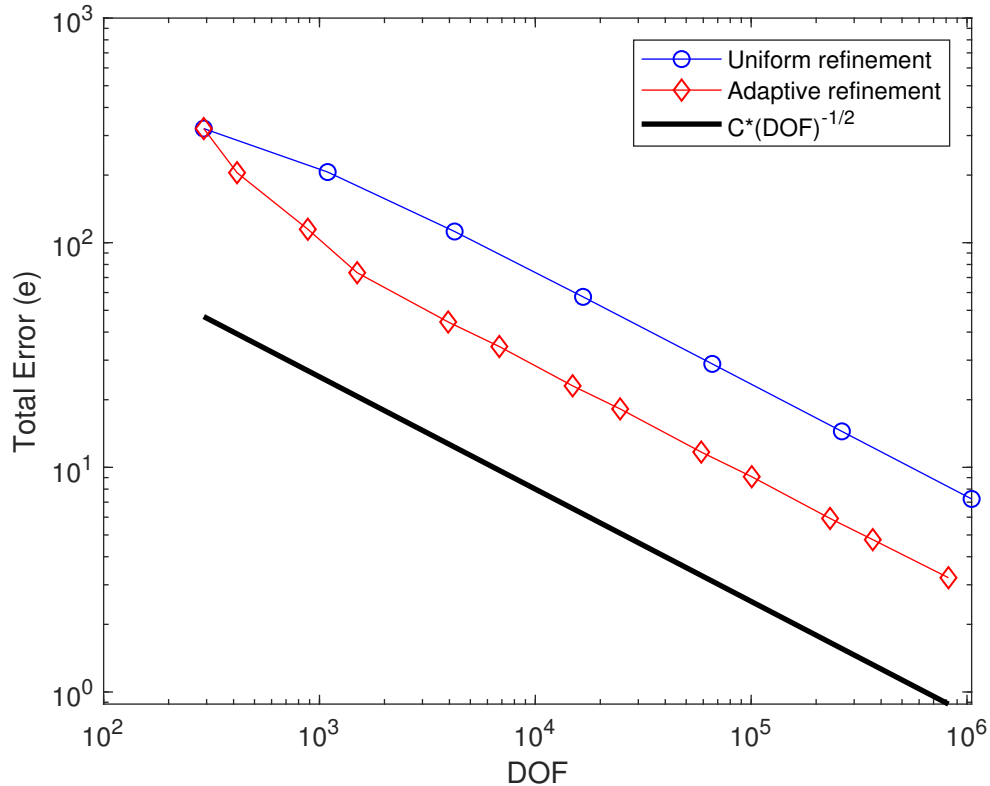


Figure 2: Total error (e) vs DOF (N) for uniform and adaptive refinements (Example 1, with $\nu = 1.0$)

- [17] P.G. Ciarlet, *The Finite Element Method for Elliptic Problems*. North-Holland, 1978.
- [18] P. Clément, *Approximation by finite element functions using local regularisation*. RAIRO Modélisation Mathématique et Analyse Numérique, vol. 9, pp. 77-84, (1975).
- [19] L. Figuera, G. N. Gatica and A. Márquez. *Augmented mixed finite element methods for the stationary Stokes equations*. SIAM Journal on Scientific Computing, vol. 31, 2, pp. 1082-1119, (2008).
- [20] G.N. Gatica, A. Márquez and M.A. Sánchez, *A priori and a posteriori error analyses of a velocity-pseudostress formulation for a class of quasi-Newtonian Stokes flows*. Computer Methods in Applied Mechanics and Engineering, vol. 200, pp. 1619-1636, (2011).
- [21] R. Hiptmair, *Finite elements in computational electromagnetism*. Acta Numerica, vol. 11, pp. 237-339, (2002).

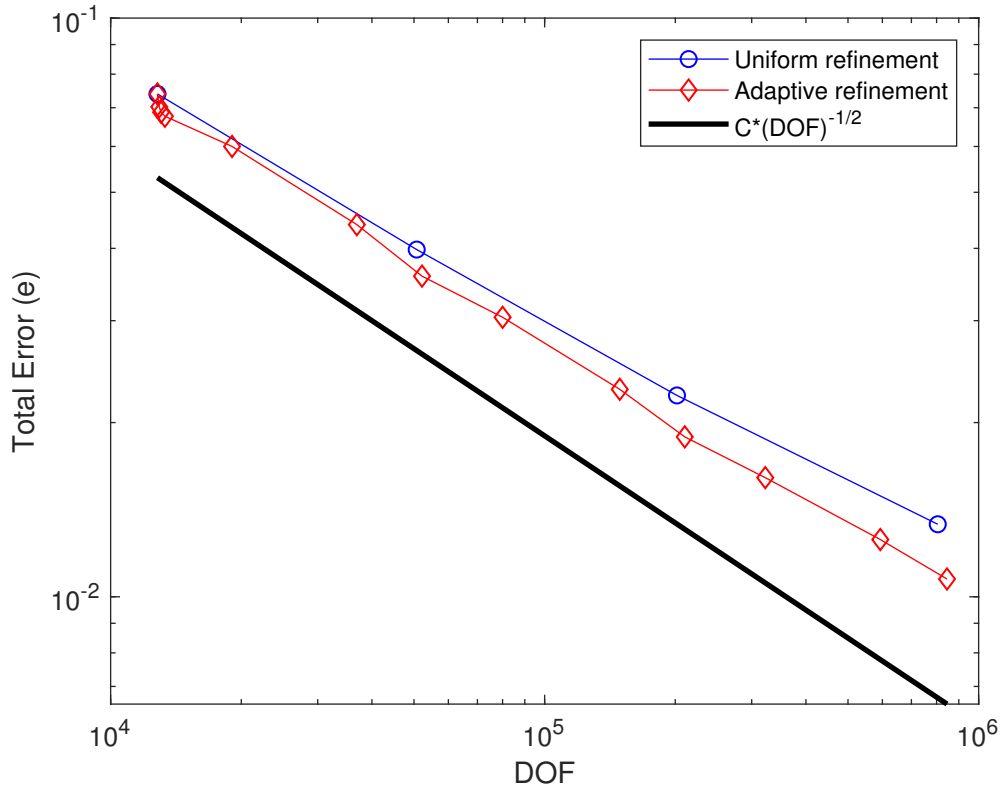


Figure 3: Total error (e) vs DOF (N) for uniform and adaptive refinements (Example 3, with $\nu = 1.0$)

- [22] L.I.G. Kovasznay, *Laminar flow behind a two-dimensional grid*, Mathematical Proceedings of the Cambridge Philosophical Society 44, no. 1, 58-62. (1948).
- [23] J.E. Roberts and J.-M. Thomas: *Mixed and Hybrid Methods*. In: Handbook of Numerical Analysis, edited by P.G. Ciarlet and J.L. Lions, vol. II, Finite Element Methods (Part 1), 1991, North-Holland, Amsterdam.
- [24] R. Verfürth, *A posteriori error estimation and adaptive mesh-refinement techniques*, J. Comput. Appl. Math. vol.50, pp. 6783 (1994).
- [25] R. Verfürth, *A Review of a Posteriori Error Estimation and Adaptive Mesh-Refinement Techniques*, Wiley-Teubner, Chichester, 1996.

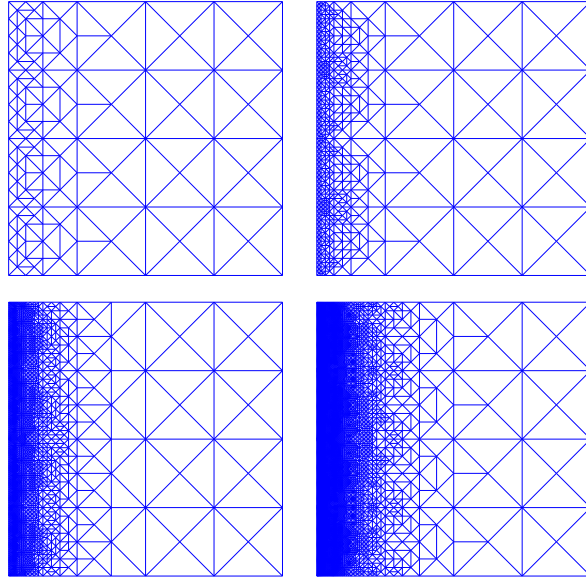


Figure 4: Adaptive refined meshes corresponding to 883, 3947, 24723 and 100623 dof (from left to right, top - bottom) (Example 2, with $\nu = 1.0$)

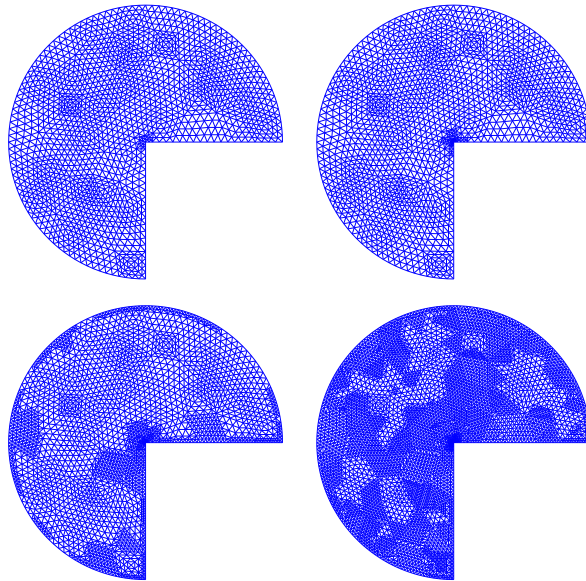


Figure 5: Adaptive refined meshes corresponding to 12943, 13339, 19045 and 36925 dof (from left to right, top - bottom) (Example 3, with $\nu = 1.0$)